Joining of thermoplastic structures by Friction Riveting: a Mechanical and a Microstructural Investigation on Pure and Glass Reinforced Polyamide Sheets

Francesco Gagliardi[1,a], Romina Conte[1,b], Claudio Ciancio[1,c], Giorgio Simeoli[2,d], Vito Pagliarulo[3,e], Giuseppina Ambrogio[1,f], Pietro Russo[2,g*]

[1]Department of Mechanical, Energy and Management Engineering, cubo 45-C, Ponte P. Bucci - University of Calabria, Arcavacata di Rende (CS) 87036 Italy

[2]Institute for Polymers, Composites and Biomaterials, Via Campi Flegrei 34 – CNR – Pozzuoli (NA) – 80078 – Italy

[3]Institute of Applied Sciences and Intelligent Systems, Via Campi Flegrei 34 – CNR – Pozzuoli (NA) – 80078 – Italy

a) francesco.gagliardi@unical.it, b) romina.conte@unical.it, c) claudio.ciancio@unical.it, d) giorgio.simeoli@unina.it, e) v.pagliarulo@isasi.cnr.it, f) giuseppina.ambrogio@unical.it, g) pietro.russo@unina.it,

* Corresponding Author

Friction Riveting is a spot joining, which consists in rotating a cylindrical rivet and inserting it into clamped sheets. In the first friction phase, the rotational speed and the applied axial force heat the material by friction plasticizing it. After that, the spindle rotation is stopped and the axial force is increased passing to the so called forging phase. Several working parameters, such as: the rotational speed, the friction and forging times, and the friction and forging pressure, have to be optimized to achieve sound connections.

In the proposed work, the attention was given to the joints of sheets made of a thermoplastic material with and without short glass fiber reinforcements. Rivets were made of Titanium Grade 2. The quality of the obtained results was verified by tensile tests. Moreover, microscopic observations were performed analysing the material deformation and integrity inside the connection volume. The influences of the monitored process parameters on the above highlighted outputs were reported providing a guideline for the process execution.

1. INTRODUCTION

In the recent years, several and different industrial sectors, such as automotive, aeronautic and power generation fields, have increased the use of multi-materials and hybrid components under the

influence of green policies and innovative manufacturing technologies. The quality of the produced components is closely linked to the connection of various parts. Briefly, joining is a complex process, which allows single parts to be assembled all together achieving specific performances in mechanical, physical and chemical terms.

The complexity of products demands for new functional processes, even if just metals have to be connected. Mori et al. [1], in 2013, spoke about plastic deformation saying that this opens to significant joining variants able to improve accuracy, reliability and environmental safety as well as to generate opportunities to design new products made of dissimilar materials.

The joining difficulties increase if materials of different classes have to be combined, adequately. For example, the limited joinability or the easy joining decline between polymers and metals are due to their dissimilarity from both a physical and a chemical point of view [2]. However, the combination of dissimilar parts can be guaranteed using different joining techniques. Martinsen et al. [3] summarized the state of the art in joining dissimilar materials classifying them in mechanical, chemical, thermal and hybrid processes. They highlighted the vastness of the topic and, therefore, described methods useful to the process selection. Haddadi and Abu-Farha [4], in 2015, stated that reaction at the interface and material incompatibilities are the most challenging barriers in joining dissimilar materials.

Traditional joining techniques, i.e. welding, adhesive bonding and mechanical fastening, need different approaches if they have to be applied to pure polymer or polymer matrix composites (PMC) instead of just metals. Among the variety of welding techniques, one of the most promising for the joining of hybrid structures is ultrasonic welding, where parts to be joined are held together under pressure and subjected to ultrasonic vibrations. This solution has been applied to join metals to both thermoplastics [5] and thermosets [6]. Concerning the interaction between these two plastic groups, Deng et al. [7], in 2015, presented a literature review with the purpose of understanding the possible mechanisms of interfacial adhesion between thermoplastics and thermosets. The review aimed to highlight the potential applications of fusion bonding in joining composite structures.

Respect to the adhesive joints, mechanically fastening solutions are, instead, free from surface treatments, and they are unaffected by the service temperature, humidity and other environmental conditions. Various solutions belong to this process category, such as bolted joints, riveting and clinching. The use of rivets or bolts has been widely analyzed to join laminates [8], too. This, however, involves the manufacturing of holes before fastening, which takes time and could cause material damage. For this reason, self-piercing rivet (SPR) has been also introduced. It allows joining of the sheets without drilling holes. Modified SPR has been proposed to minimize delamination at the points of piercing [9]. Furthermore, multi bolted joints have been investigated as a valuable solution to improve the obtainable connection strength [10]. According to that, numerical models have been

developed to predict failure load and failure modes of mechanically fastened composite joints giving mathematical tools to judge the various solutions, theoretically [11].

Clinching is another family of processes, which does not require preliminary drilling of the sheets to be joined. Furthermore, this family enables further advantages, as it does not need additional joining elements, which would bring to higher costs as well as to increase the part weight. Lambiase and Ko, in 2017 [12], investigated two-steps clinching, where a reshaping deformation is used at the end of the clinching phase to improve the mechanical behavior of the connections.

The continuous research of improving the joining quality has pushed the research to combine various techniques, too. For example, Mucha [13], in 2011, proposed a hybrid joining process with the superposition of a mechanical joint to an adhesively bonded joint. Overall, it has been found that the strength of properly designed hybrid bolted/bonded joints is higher than bolted or bonded joints alone. In this direction, Lopez-Cruz et al. [14], in 2017, proposed a design of experiments to point out the performance of bolted/bonded composite joints by considering several design variables at the same time. In this way, the combination of various effects was observed.

Nevertheless wide joining solutions, new designs and materials have been pushing to new techniques. Thermoplastic composites emerged in the last years because of their properties and for high-end applications respects to thermosets [15]. Abibe et al. [16], in 2011, described the principles of Injection Clinching Joining (ICJ) analyzing the process variables, the quality of the connections and the potential applications. In this solution, a stud is produced from the surface of the thermoplastic sheet and fits into a machined profiled hole on the part to be joined. Friction Lap Joining (FLJ) [17] is another novel connection method able to join plastic materials, carried out with a similar equipment of Friction Stir Welding [18]. FLJ uses the heat produced by friction between a rotating rigid tool and a metal surface to produce a narrow melted region in the joined plastic near the interface. Friction Spot Joining (FSpJ) [19] also utilizes a not consumable tool to perform connections. However, in this case, the tool consisting of three parts, whose movements, coordinated properly, are used to plasticize a volume of material by friction, which is then pushed and pressed to generate a spot connection. Amancio Filho patented a new spot joining process known as Friction Riveting (FricRiveting) [20]. This technique uses a cylindrical metallic rivet to connect thermoplastic-metal parts plasticizing and deforming the tip of the rotating rivet heated by frictional forces. Before the joining phase starts, a specific equipment clamps the sheet to be connected, firmly. The process, performed by a high-speed friction welding system, is divided in two different phases. During the first one, known as heating phase, the metallic rivet, rotating, gets into the components to be joined. At the end of this phase, there is a deceleration of the rotational speed and the rived is pushed into the material to be connected. This is called forging phase. The FricRiveting temperatures are usually found to lie within the early stage of degradation of the investigated thermoplastics [21]. Various variables, such as the rotational

speed, the friction time and the friction pressure, the forging time and the forging pressure, have to be combined properly to optimize the quality of the connection. A better understanding of the mechanical behavior of the joint can be reached by numerical analyses, which are quite complex to perform taking into account the metal-plastic interaction. The first attempt on that was performed by simulating joints made of polyetherimide sheet and AA2024-T351 rivets using the commercial code Abaqus [22]. The feasibility of Friction Riveting on thermoplastic composites has been proved considering plastic matrixes reinforced with short fiber [23] and laminates [24]. High-performance plastics, i.e. Polyetherimide (PEI) and poly-ether-ether-ketone (PEEK) [22–25] have been usually investigated, while just a research has been focused on polycarbonate [26], which belongs to engineering plastics generally characterized by lower mechanical properties. This is relevant to the FricRiveting dynamics being the rivet tip deformed at the end of the process for a right combination of temperature and plastic resistance during the forging phase. Both of the highlighted variables are affected by the mechanical and thermal properties of the materials of the parts to be connected.

In the work here proposed, FricRiveting was used to join an engineering plastic, polyamide 6 with and without glass fiber reinforcement. The feasibility of the process was proved using a customized equipment and a traditional milling machine and the influence of various process parameters on the quality of the connection was investigated. According to that, tensile tests were performed to judge the anchoring of the rivet with the sheet. Furthermore, preliminary analyses were carried out to evaluate the influence of the process parameters on the strain distribution of the worked polymer around the joining area. These tests used an Electronic Speckle Pattern Interferometry (ESPI) or rather an interferometric non-destructive testing technique that works in full-field modality [27,28]. Finally, optical observations have been performed to judge the integrity of the material in the same area.

2. MATERIAL, EQUIPMENT AND METHODS

2.1 Materials

The research involved sheets based on polyamide 6 (PA6): an engineering thermoplastic used in several sectors going from construction to lighting, from automotive to aviation industries, and so on [29,30]. It is characterized by mechanical properties allowing light components to be designed and manufactured, for instance, for the transport sector, where the weight reduction is one of the main priority [31]. In details, raw plastic materials were commercial grades supplied by Lanxess (Cologne, Germany) under the trade names Durethan B30S (MFR: 125.5 g/10 min@260 °C/5Kg, d: 1.14 g/cm^3) and Durethan BKV30 H (MFR: 18 g/10 min@260 °C/5Kg, d: 1.36 g/cm^3). The former is a white virgin grade PA6 resin while the latter is a black grade containing 30 wt% of glass fibers and a low

content of carbon black usually included in formulations for the automotive field just for aesthetic reasons.

The rivets, with a length of 60 mm and a diameter of 5 mm, instead, were constituted by titanium grade 2: a commercially pure titanium alloy with high specific strength and good corrosion resistance. Table 1 reports the main mechanical and thermal properties of the materials used in the performed research. Concerning PA6, ranges of variability have been reported according to the literature [32] for those properties whose values are not provided by the producer.

Table 1: mechanical and thermal properties of the investigated raw materials.

Material	Density (g/cm^3)	Young's Modulus (GPa)	Tensile Strength (MPa)	Thermal Conductivity (W/mK)	Spec. Heat Capacity (J/g °C)	Melting Temperature (°C)
PA6 Durethan B30S	1.14	1.1	20-142	0.23-0.35	1.50 - 1.70	210-220
PA6 Durethan BKV30 H	1.36	6.1	28-285	0.20-1.64	0.35-2.43	208-315
Ti Grade 2	4.51	102	430	16.40	0.523	166

2.2 Sheet preparation

The sheets to be joined were obtained by compression molding by using a Lab Press Colin GmbH (Edersberg, Germany) mod. P400E. PA6 based resins, dried at 80 °C for 3 h, were molded in 5 mm thick sheets under the temperature and pressure profiles shown in the following Fig. 1.
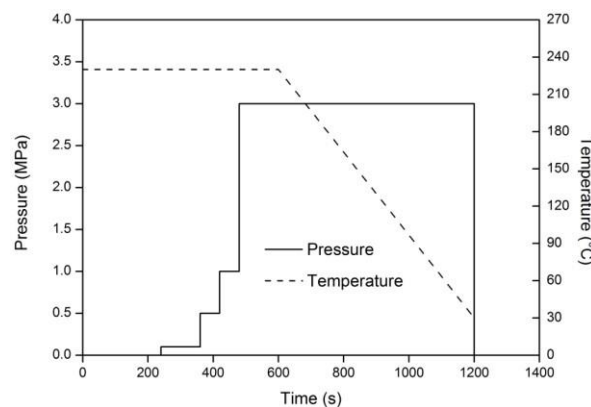
Figure 1: compression molding conditions.

2.3 Equipment

The feasibility of FricRiveting was proven without using a dedicate friction welding system [19–26]. In detail, a milling machine was utilized to carry out the planned experiments. The process variables change and, as doing, the rivet stroke becomes a variable to be controlled and the loads during the process are, instead, outputs to be measured. The required high spindle speeds necessary to perform the process were reached by a speed multiplier, which is placed inside the milling mandrel allowing the imposed set value to be quadrupled, up to 40000 rpm. Therefore, the spindle speed is properly increased in order to get a desired temperature increment during the heating phase. Furthermore, a suitable equipment was designed and located inside the working volume of the machine. This equipment was used to maintain solidly blocked the sheets during the working phase. Two sheets with a thickness of 5 mm were joined. The equipment was placed on a dynamometer to monitor the loads during the process at various working conditions. Finally, a thermocouple and a thermo-camera were utilized to check the temperature trend during the process. The thermocouple was embedded in pre-defined positions chosen taking into account the experimental evidences, highlighted in [20], where it was noticed how the temperature trend, locally measured, presented consistent differences according to the position of the thermocouple along the specimen thickness (z-axis). The center of the upper sheet was the selected position to embed the thermocouple with the depth of the hole that was fixed with a distance of around 1 mm between the tip of the measuring tool and the external surface of the rivet. The experimental equipment is reported in Fig. 2.
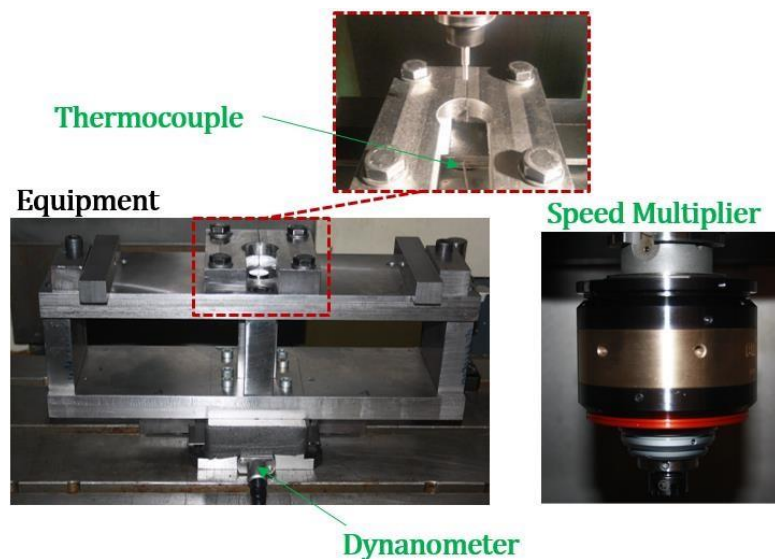
Figure 2: equipment utilized for the performed experiments.

2.4 Monitored outputs and investigated process variables

The process dynamics are well understood. The first phase of the process has to guarantee the production of a specific amount of heat around the tip of the rivet in a specific time. This heat has to increase the ductility of the metallic rivet, which as doing, during the second process phase, can be

forged properly. The desired deformation can be reached pushing the rivet against a material, pure or reinforced thermoplastic, which being further from the heated zone and characterized by a low conductivity, is at lower temperature and with more elevated mechanical properties. Therefore, a compromise between reached temperature (and its associated effects on the thermoplastic rheology that determines the resistance to the rivet penetration) and forging force needs to be found for each combination of rivet and sheets to be connected. For this reason, recorded temperature and forging forces were the outputs quantitatively measurable that, together with the maximum strength required to pull out the rivet from the sheets, were used in a proposed mathematical procedure to identify the optimal combination of process parameters.

In particular, the maximum pulling strength was measured by tensile tests performed on an Instron testing machine with a traverse speed of 1 mm/min at room temperature and with a load cell of 5 kN. The connected parts were tested fixing them in a sample holder made of two bolt-connected rigid plates, while the rivet is clamped to the moving traverse and pulled out from the sheets (Fig. 3). Due to the complex geometry of the deformed rivet, the determination of a real cross-sectional rivet area was very difficult and, consequently, the joint strength is presented only in terms of tensile force.
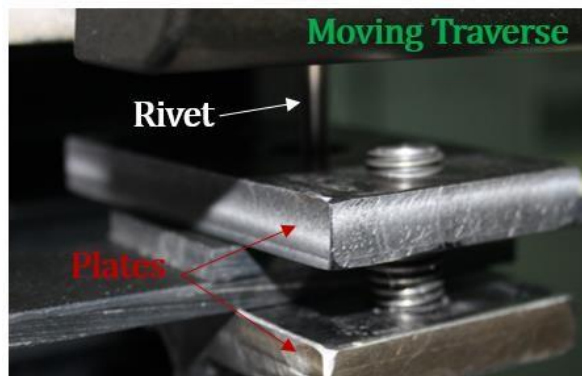
Figure 3: the specimen fixed in customized holder inside the volume of the tensile test machine.

Furthermore, ESPI technique was used to qualitatively investigate the out of plane displacements of stressed specimens and in such way enabled to identify cracks and strains on rough surfaces with high sensitivity in real time, without contact and in full field modality. In general, the detection of microdeformations is possible illuminating the surface by a visible laser (i.e. wavelength 532 nm) and the measurement accuracy is related to this wavelength. A CCD camera records two states (deformed and non-deformed) and electronically subtracts them: in such a way, the deformation is shown under correlation fringes form and subsequently as phase-contrast map, which the displacement field with high accuracy is measured from. The deformation is usually obtained imposing a slight warming to the material.

The experimental campaign was carried out working thermoplastics with or without a percentage of glass fiber reinforcements and taking into account the parameters reported in Table 2. In detail, the spindle speed, the rivet linear velocity, divided between friction and forging phases, and the rivet linear stroke during the forging phase were monitored. Concerning the last reported variable, this was related to the rivet linear stroke during the friction phase being the thickness of the sheets to be joined fixed and equal to 10 mm and providing a total stroke of the rivet, considering both friction and forging phase, of 9 mm.

Table 2: process and material variables investigated in the performed analysis.

Linear Velocity - Friction [mm/s]	Linear Velocity - Forging [mm/s]	Linear Stroke Forging [mm]	Spindle Speed [RPM]	Glass Fiber [%]
1.0	1.0	3.0	15000	0
2.0	2.0	4.5	25000	30
3.0	3.0	6.0	35000	

3. MATHEMATICAL PROCEDURE TO IDENTIFY THE OPTIMAL COMBINATION OF PROCESS PARAMETERS

The objective of the proposed method is to identify the most significant process parameters that influence the value of three output responses quantitatively measured (i.e. reached temperature, forging load and pulling strength). The main objective is to give some guidelines on how to maximize the quality of the obtained joint. However, it is also useful to analyze the impact of different approaches on other process responses that could limit the applicability of some process configurations. The number of required experiments was reduced utilizing a mathematical procedure. The main steps of the implemented approach are:

1. *Definition of the process domain*: the set of factors that influence each key performance indicator is determined in accordance with literature [19–26]. As a result, the process parameters indicated in Table 2 were selected and the range of values to consider was defined.

2. *Definition of the Design of Experiments*: a crucial role on the quality of a predictive model is given by the choice of the design of experiment. A Taguchi design was used since it offers a good trade-off between accuracy and costs.

3. *Feature selection*: the collected data are used to identify the set of process parameters that influence any output response. The Regressional ReliefF (RReliefF) [33] method was used for this task.

4. *Definition of the optimal process configuration*: the configuration that maximizes the quality of the obtained joint is identified. Different configurations could be defined according to the required constraints that the user has to take into account for the specific application. Each step of the proposed procedure is described in the following section, where it is presented how the methodology was applied on the case study.

3.1 Design of Experiment

The first step to perform a statistical investigation of a mechanical process is to define the boundaries of the analysis fixing a lower-upper value of each investigated feature. To this aim, the main process parameters and their ranges were chosen as reported in Table 2. Subsequently, it was necessary to define the sampling strategy to collect a set of data to test and train the model.

Instead of a full factorial design [34], which would require 486 (3^5*2) tests, a fractional design was used to decrease significantly the number of the required data saving a considerable amount of time and costs. To this aim, the Taguchi method [35] uses a special design of orthogonal arrays to study the entire space of parameters with a small number of experiments. A set of fractional factorial designs ignores the parameter interactions and focuses the attention on the estimation of the main effects. This design is particularly suitable for initial analysis in which the main goals are a first understanding of the system and a screening of the most relevant variables for each process indicator.

The steps included in the Taguchi methodology are:

1. selecting the proper orthogonal array (OA) according to the number of parameters;
2. running experiments based on the selected OA;
3. analyzing data;
4. identifying the optimum process conditions.

The array chosen for this application is the L_{27} [35], which has 27 rows corresponding to the number of tests and can be used to analyze a number of parameters up to 13. The design was performed with two replications to check the process replicability carrying out a more reliable statistical analysis. The number of experiments performed was therefore equal to 54.

3.2 RReliefF Method

A Feature selection technique has been utilized in this study to identify the most influent process parameters. Feature selection focuses on eliminating redundant and irrelevant data and is a crucial part of preprocessing step to determine more accurate input-output relationships. In few words, feature selection improves the quality of the data and increases the performance of metamodel algorithms by reducing the space and time complexity. In this research, the RReliefF technique was

used to select the relevant features of each investigated process objective. Relief algorithms are general and successful attribute estimators. They are commonly viewed as feature subset selection methods applied in a pre-processing step before the model is learned, and are among the most successful pre-processing algorithms. RReliefF algorithm estimates the quality of attributes by how well their values distinguish between patterns that are near to each other. It was assumed that examples $I_1, I_2, ..., I_n$ in the instance space are described by a vector of attributes A_i, $i = 1,...,a$, where a is the number of attributes, and are labelled with the target value τ_i. The main idea of the algorithm is to calculate the importance of each attribute $W[A]$. The value $W[A]$ is calculated based on the estimation of P_{diffA}, P_{diffC}, $P_{diffC|diffA}$:

$$P_{diffA} = P(\text{diff value of } A | \text{nearest instance})$$

$$P_{diffC} = P(\text{different prediction} | \text{nearest instance})$$

$$P_{diffC|diffA} = P(\text{different prediction} | \text{diff value of } A \text{ and nearest instance})$$

The value of $W[A]$ is calculated based on Bayesian rule as:

$$W[A] = \frac{P_{diffC|diffA} P_{diffA}}{P_{diffC}} - \frac{(1 - P_{diffC|diffA}) P_{diffA}}{1 - P_{diffC}}$$

The algorithm is expressed as follows where the weights for different prediction, different attribute, and different prediction & different attribute are denoted as N_{dC}, $N_{dA}[A]$, $N_{dC\&dA}[A]$, respectively:

Algorithm RReliefF

Input: for each training instance a vector of attribute values x and its predicted value $\tau(x)$ *Output*: vector W of estimations of the qualities of attributes

1. **Set** all N_{dC}, $N_{dA}[A]$, $N_{dC\&dA}[A]$, $W[A]$ to 0
2. **for** i:=1 to m **do begin**
3. randomly select instance R_i;
4. select k instances I_j nearest to R_i;
5. **for** j:=1 to k **do begin**
6. $N_{dC} := N_{dC} + \text{diff}(\tau(\cdot), R_i, I_j) \cdot d(i,j)$;
7. for A:=1 to #attributes do begin
8. $N_{dA}[A] := N_{dA}[A] + \text{diff}(A, R_i, I_j) \cdot d(i,j)$;
9. $N_{dA\&dA}[A] := N_{dA\&dA}[A] + \text{diff}(\tau(\cdot), R_i, I_j) \cdot \text{diff}(A, R_i, I_j) \cdot d(i,j)$;
10. **end**
11. **end**
12. **end**
13. **for** A:=1 to #attributes **do**

14. $W[A] = N_{dA\&dA}\,[A]/\,N_{dC} - (\,N_{dA}[A] - N_{dA\&dA}[A])/(m - N_{dC})$; The value diff(A, $R_{i,}I_j$) is calculated as:

$$\text{diff}(A, Ri,, Ij) = \frac{|value(A, R_i) - value(A, I_j)|}{\max(A) - \min(A)}$$

The term $d(i,\text{j})$ calculates the distance between the two instances $R_{i,}$ and I_j. The ratio is that closer instances should have a greater influence, so the influence of the instance I_j with the distance from the given instance R_i is exponentially decreased:

$$d^{(i,j)} = \frac{d_1\,(i,j)}{\sum_{l=1}^{k} d_1(i,l)}$$

$$d_1(i,l) = e^{-\left(\frac{Rank(R_i,I_j)}{\sigma}\right)^2}$$

where, $Rank(R_i,\,I_j)$ is the rank of the instance I_j in a sequence of instances ordered by the distance from R_i and σ is an algortithm predefined parameter used to control the influence of the distance. The final estimation of the relevance of each attribute $W[A]$ is finally computed through the expression in line 14 of the algorithm.

The threshold value to select the relevant features can be determined by Chebyshev's inequality for a given confidence level α (where α is the probability of accepting an irrelevant feature as relevant) and it is equal to $\frac{1}{\sqrt{\alpha \cdot m}}$. However it is stated that a much smaller value could be used [33]. Therefore, we define as "secondary relevant parameters" the features with a value $W[A]$ in the range $\left[\frac{1}{2\sqrt{\alpha \cdot m}}, \frac{1}{\sqrt{\alpha \cdot m}}\right]$.

4. RESULTS AND DISCUSSION

The rivet, due to the spindle rotation, enters inside the thermoplastic and completes the joining phase with its deformation anchoring to the sheets. A barreling of the rivet, more or less pronounced, can be observed (Fig. 4a).

No external deformation of the rivet is, instead, noticeable. Regarding the upper surface of the joining, the processed thermoplastic material surrounds the stick of the rivet forming a flash that can have different shape and aspect. The plastic, in fact, during the process is firstly stirred and locally heated and, then, compressed during the forging phase. According to the reached temperatures, the polyamide touches different levels of viscosity and, therefore, the surface of the flash can be more grainy or more shiny according to the reached working temperatures (Fig. 4b and 4c).
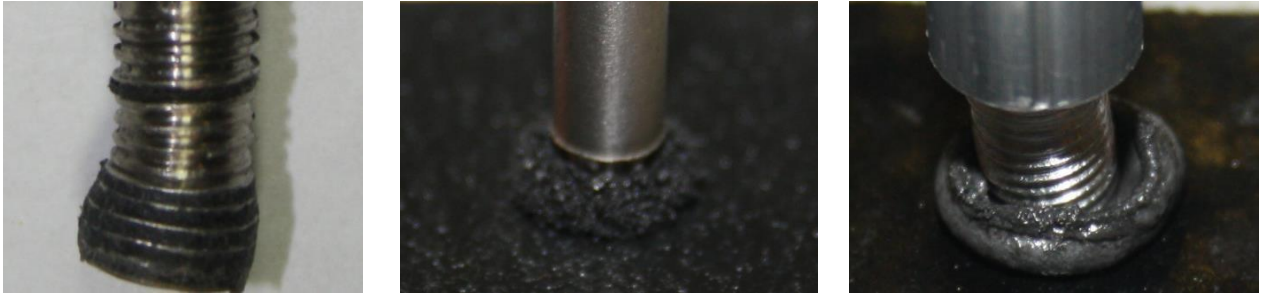
Figure 4: a) a pulled out rivet and b) a grainy and c) a shiny flash surface.

Regarding the temperature monitored during the process, the thermo-camera catches the values all around the working volume with the flash area, which is, as expected, the hottest zone (Fig. 5). In particular, temperature picks of more than 300°C were recorded for various process configurations.

300°C

225°C

150°C

75°C

20°C
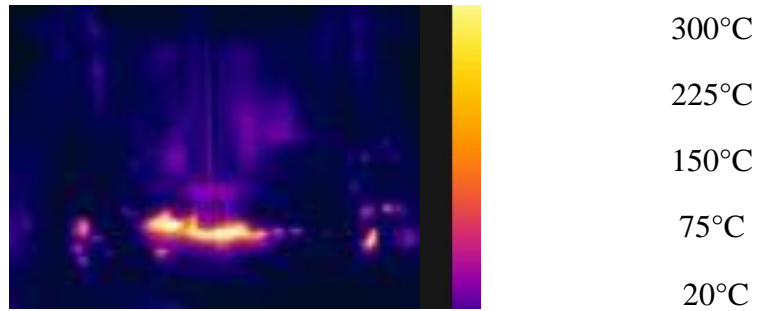
Figure 5: thermal infrared image at the end of friction phase.

The thermocouple, instead, gives information about the temperature trend inside the joined sheets. The maximum value revealed by this measurement device according to its fixed position was close to 60°C, resulting significantly different from those recorded by the thermo-camera. This fact can be justified taking into account that the temperature values obtained by the thermocouple depending on its position inside the joining volume [20]. Due to the wider recorded spectrum, the data obtained by the thermo-camera were utilized for the optimization of the process conditions. A summary of the main results achieved through the proposed design is reported in Table 3.

Table 3: Design of Experiments: experimental results.

Process Responces	Minimum Value	Maximum Value
Forging Load, N	2438	4728
Temperature, $°C$	302	456
Strength, N	147	2429

4.1 The statistical outcomes

The RReliefF was performed using a number of iteration *m* equal to 27 (number of data) and a level of confidence of 90% (α=0.1). Therefore, a main threshold equal to ≈0.2 and a secondary limit equal to ≈0.1 are fixed. The importance of each attribute $W[A]$ and the main effect are reported for all the three process responses in Table 4 and Fig. 6 . The plot represented in Fig. 6 considers a normalized value in the range [0,1] to avoid different units of measure.

Forging load: this variable is mainly influenced by the rivet stroke. As above highlighted, this variable is fixed between friction and forging phase, whose combination brings to a total rivet movement of 9 mm. The required force increases if the stroke during forging increases and, consequently, the friction phase is shorter. In fact, as expected, the force is low during the friction phase and increases steeper once the punch dips inside the composite sheets during the forging time (Fig. 7). Longer is this time, higher, for the same working conditions, is the peak of the monitored force. The joined material is the secondary variable, which has to be considered to control the process force. In the performed experiments, this means that the forging force increases for glass fiber reinforced sheets. The other monitored inputs, instead, have a reduced influence on the discussed output as clearly highlighted in Table 4.

Table 4: relevance of the investigated variables on the monitored outputs.

Process Parameter	Forge Load	Strength	Temperature
Linear Velocity Friction	0.069	0.067	0.205
Linear Velocity Forging	0.061	0.091	0.203
Linear Stroke Friction	0.297	0.122	0.056
Spindle Speed	0.088	0.272	0.118
Material	0.135	0.209	0.080
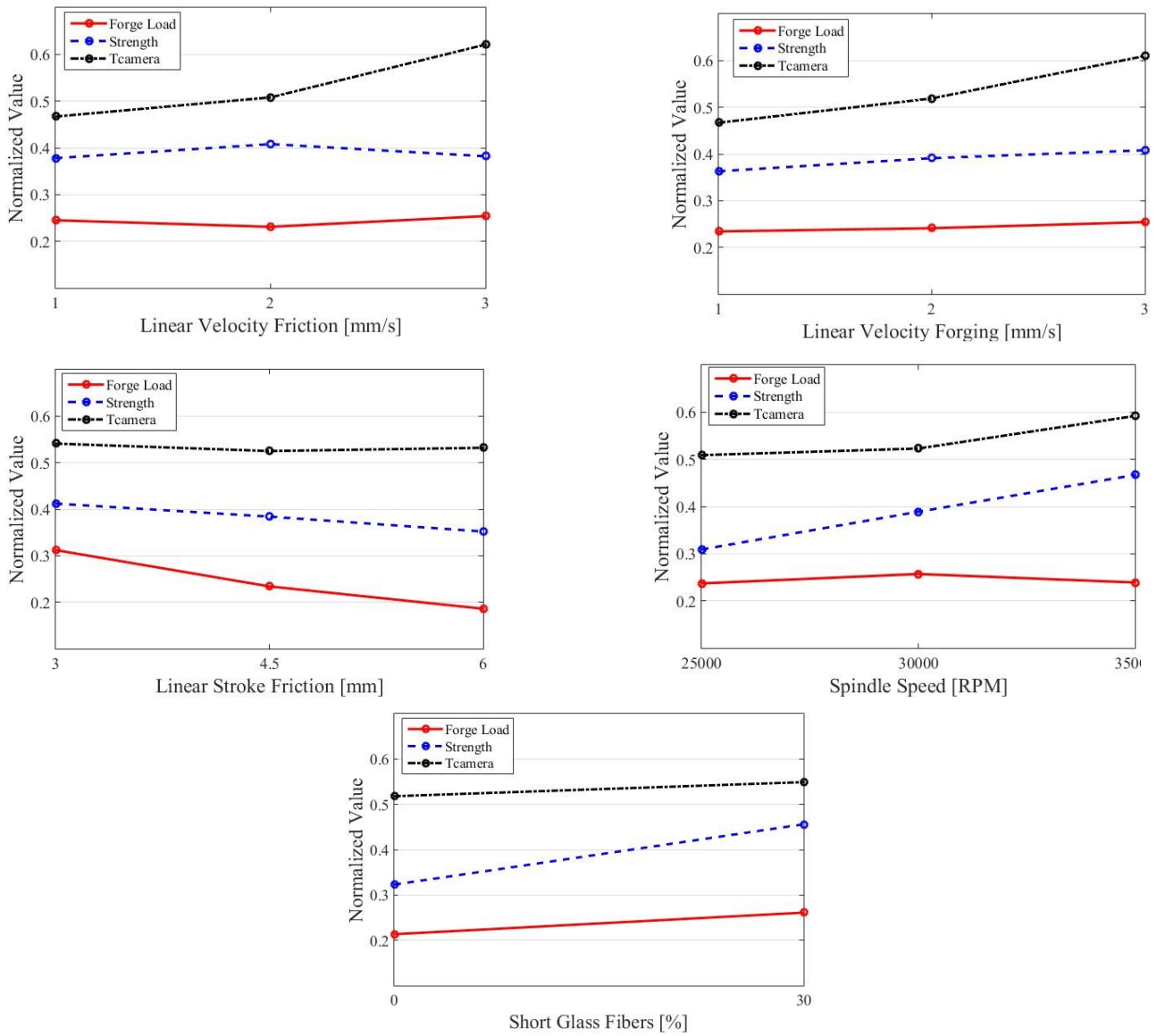
Figure 6: the influence of the investigated variables on: forging forces (F-Force), recorded temperature (T-Camera) and maximum strength (Max-Strength).
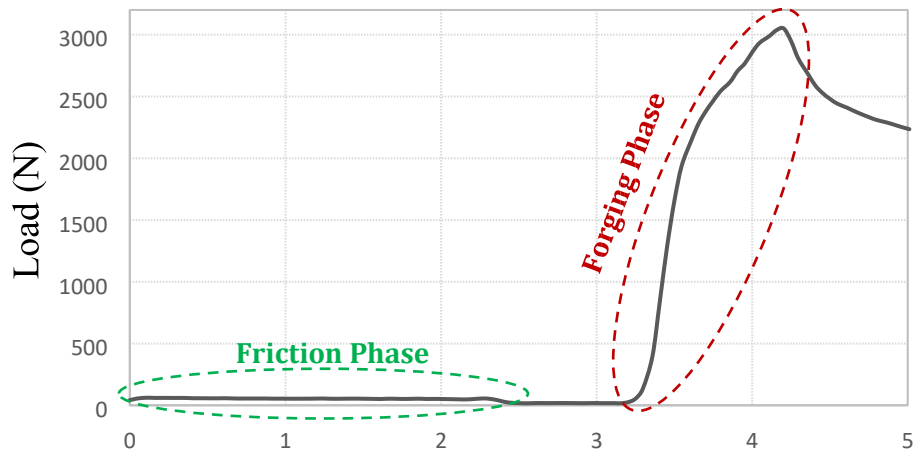
Time (s)

Figure 7: force trend during the process.

Temperature: the maximum temperature reachable in the process depends on the heat produced during the friction phase. This consideration is confirmed from the obtained results. In fact, looking at Fig. 6 and Table 4, both the friction linear velocity and stroke affect the temperature monitored by the utilized thermo-camera. In detail, the friction linear velocity seems to be the most meaningful variable and the achievable temperature is higher for more elevated rivet speed. This result could be explained because, if the heating phase is reduced due to the velocity increment of the joining tool, the heat dispersion decreases. This effect is further increased if elevated forging linear velocities are set. Anyway, the highlighted evidence has to be further proved with additional experiments. As said, in fact, the designed statistical plan gives preliminary understandings of the variable relevancies, but the parameter interactions can provide a clearer view on the process dynamics. The spindle speed is the other variable, which contributes meaningful to the temperature variation. A higher spindle speed increases the revolutions of the rivet inside the plastic matrix, increasing the heat produced by friction and, consequently, the temperature variation. Even for this output, the other monitored inputs do not show noteworthy influence.

Strength: the tensile strength required to pull out the rivet from the composite sheets depends on the joined material. This is explainable considering that, during the tensile test, the material is deformed to allow the rivet to be removed from the connection zone. The other relevant input, which affects the joining quality, is the spindle speed, which is important to heat the metallic part before the forging phase and, therefore, increasing its ductility which improves the material formability. Indeed, at least for these first reported evidences, the linear velocity of the rivet during the friction phase has a relevant effect on the temperature variation monitored by the thermo-camera. The reduced influence of this variable on the tensile strength of the joint can be, however, explained taking into account that, if this velocity increases the contact time between the molten polymer and the rivet, proportionally decreases and this goes to reduce the temperature of the metal before its forming. Finally, the stroke of the rivet during forging results to be meaningful to the quality of the connection. This is understandable taking into account the link between stroke and forging force. An increment of the last variable due to a longer forging phase, in fact, brings to a more consistent rivet deformation.

4.2 ESPI analysis and microscopic observations

Finally, a preliminary analysis was carried out by ESPI and optical microscopy to highlight the influences that glass fiber percentage and spindle speed have on the out of plane displacements around the joining area. These two variables were selected considering their consistent impact on the monitored process outputs as shown in the previous section.

The strain distributions on the upper sheet surface of specimens based on pure and glass fiber filled polyamide, processed under same conditions, are reported in Fig. 8. In this case, it seems that no substantial differences are induced in terms of deformations and no cracks have been revealed on the edge if elevated spindle speed (35000 rpm) is utilized (see Fig. 8a and b). This consideration is confirmed by optical micrographs (Fig. 8c and d).

In Fig. 9, instead, images related to specimens containing 30% by weight of glass fibers, but processed under different spindle speed are reported. In particular Fig. 9a and 9b show the phase contrast maps obtained by ESPI on specimens subjected to spindle speed of 20000 rpm and 35000 rpm, respectively.
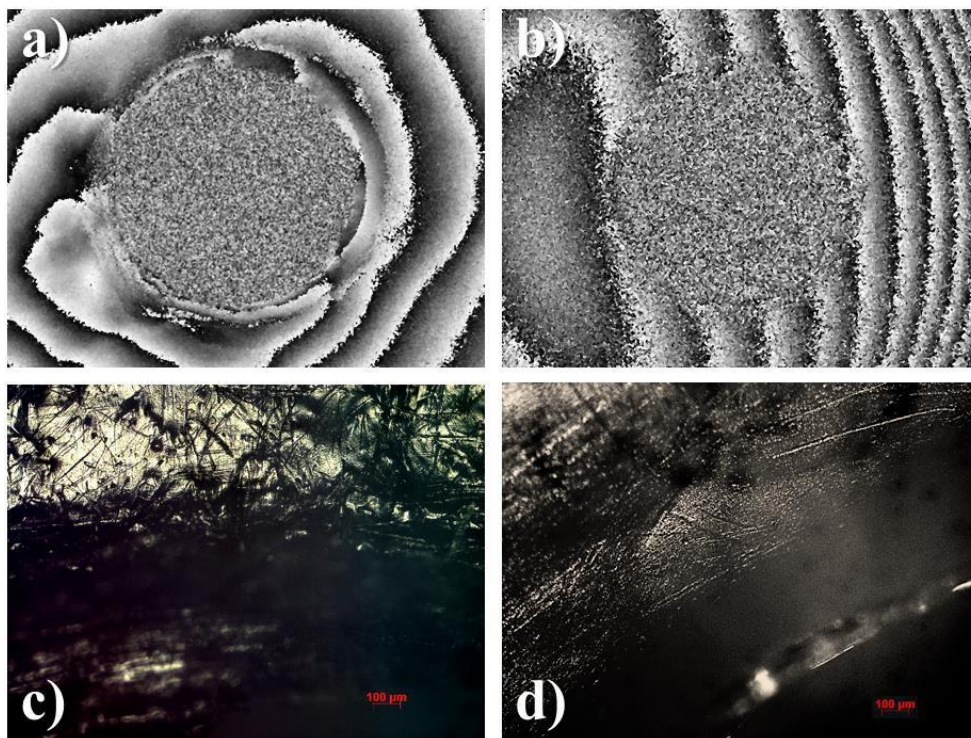
Figure 8: Phase-contrast map obtained by ESPI after a thermal stimulation for a) "pure" specimen and b) "30%FV" specimen. Images from optical microscope: c) part of the edge of "pure" sheet and d) part of the edge of a "30%FV" sheet.
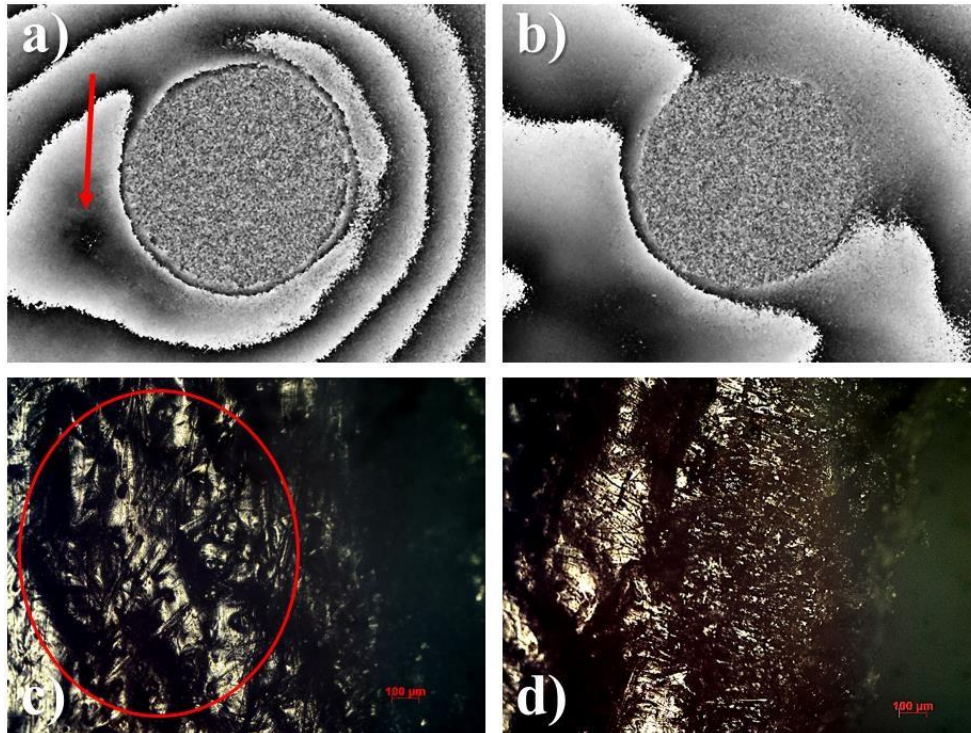
Figure 9: Phase-contrast map obtained by ESPI after a thermal stimulation at a) 20000 rpm and b) 35000 rpm. Correspondent optical microscope images for specimen processed with a spindle speed equal to c) 20000 rpm and d) 35000 rpm.

The analysis shows a notable influence of the rotational speed parameter on the quality of the obtained holes. In particular, while the one in Fig. 9b appears with a good quality, in the case of lower spindle speed, Fig. 9a, the red arrow highlights an inhomogeneous deformation around the hole edges. The microscope image shown in Fig. 9c confirms in such zone (red circle) the presence of a mass thickening. This effect could be ascribed to the moving and adjustment difficulties of the plastic matrix during the rivet insertion due to the higher material viscosity because of fiber presence and lower working temperatures. This conclusion, which needs more investigation, was, however, further supported considering that the highlighted inhomogeneity was not registered if pure PA sheets are joined at any spindle speeds.

5. CONCLUSIONS

Friction riveting is a relatively new variant of mechanical fastening, which can be used to join highperformance plastics using a specific friction welding system. In the proposed research, a traditional milling machine was properly equipped and utilized to join engineering plastics characterized by lower mechanical properties and temperature degradation. In particular, the

experimental campaign highlighted the influence of different process parameters on the performed joints, whose quality was evaluated by tensile tests.

The importance of the spindle speed to increase the process performance was proved. In fact, this is the process variable that, depending on the percentage of the glass fiber reinforcement, mainly affects the anchoring force of the rivet inside the connected parts. The relation between spindle speed and material properties was also shown looking at the strain distribution and material deterioration on the upper joined surface. In particular, the material strain around the rivet area is characterized by different degrees of no uniformity depending on the spindle speed values and the used percentages of glass fibers while no thermal degradation was detected. In specific, if a lower spindle speed is used to join short fiber composite sheets, no uniformity strain distributions are generated around the hole edges. These strain distributions have to be properly taken into account because they can be responsible of material damage rising.

In conclusion, the importance of the spindle speed on the integrity of the performed joints can be understood considering that the highlighted strain inhomogeneity was not observed for higher values of this process parameter, even if reinforced plastics are processed.

6. REFERENCES

[1]   Mori K, Bay N, Fratini L, Micari F, Tekkaya AE. Joining by plastic deformation. CIRP Ann 2013;62:673–94. doi:10.1016/j.cirp.2013.05.004.

[2]   Amancio-Filho ST, dos Santos JF. Joining of polymers and polymer-metal hybrid structures: Recent developments and trends. Polym Eng Sci 2009;49:1461–76. doi:10.1002/pen.21424. [3] Martinsen K, Hu SJ, Carlson BE. Joining of dissimilar materials. CIRP Ann 2015;64:679–99. doi:10.1016/j.cirp.2015.05.006.

[4]   Haddadi F, Abu-Farha F. Microstructural and mechanical performance of aluminium to steel high power ultrasonic spot welding. J Mater Process Technol 2015;225:262–74. doi:10.1016/j.jmatprotec.2015.06.019.

[5]   Magin J, Balle F. Solid state joining of aluminum, titanium and their hybrids by ultrasonic torsion welding. Materwiss Werksttech 2014;45:1072–83. doi:10.1002/mawe.201400355.

[6]   Lionetto F, Balle F, Maffezzoli A. Hybrid ultrasonic spot welding of aluminum to carbon fiber reinforced epoxy composites. J Mater Process Technol 2017;247:289–95. doi:10.1016/j.jmatprotec.2017.05.002.

[7]   Deng S, Djukic L, Paton R, Ye L. Thermoplastic–epoxy interactions and their potential applications in joining composite structures – A review. Compos Part A Appl Sci Manuf 2015;68:121–32. doi:10.1016/j.compositesa.2014.09.027.

[8]   Thoppul SD, Finegan J, Gibson RF. Mechanics of mechanically fastened joints in polymer–matrix composite structures – A review. Compos Sci Technol 2009;69:301–29. doi:10.1016/j.compscitech.2008.09.037.

[9]   Ueda M, Miyake S, Hasegawa H, Hirano Y. Instantaneous mechanical fastening of quasiisotropic CFRP laminates by a self-piercing rivet. Compos Struct 2012;94:3388–93. doi:10.1016/j.compstruct.2012.04.027.

[10]   Yun J-H, Choi J-H, Kweon J-H. A study on the strength improvement of the multi-bolted joint. Compos Struct 2014;108:409–16. doi:10.1016/j.compstruct.2013.09.047.

[11]   Zhang J, Liu F, Zhao L, Fei B. A novel characteristic curve for failure prediction of multi-bolt composite joints. Compos Struct 2014;108:129–36. doi:10.1016/j.compstruct.2013.09.019. [12] Lambiase F, Ko D-C. Two-steps clinching of aluminum and Carbon Fiber Reinforced Polymer sheets. Compos Struct 2017;164:180–8. doi:10.1016/j.compstruct.2016.12.072.

[13]   Mucha J. The analysis of lock forming mechanism in the clinching joint. Mater Des 2011;32:4943–54. doi:10.1016/j.matdes.2011.05.045.

[14]   Lopez-Cruz P, Laliberté J, Lessard L. Investigation of bolted/bonded composite joint behaviour using design of experiments. Compos Struct 2017;170:192–201. doi:10.1016/j.compstruct.2017.02.084.

[15]   Baird, D G & Collias DI. Polymer processing: principles and design. 2014.

[16]   Abibe AB, Amancio-Filho ST, Dos Santos JF, Hage E. Development and Analysis of a New Joining Method for Polymer-Metal Hybrid Structures. J Thermoplast Compos Mater 2011;24:233– 49. doi:10.1177/0892705710381469.

[17]   Nagatsuka K, Yoshida S, Tsuchiya A, Nakata K. Direct joining of carbon-fiber–reinforced plastic to an aluminum alloy using friction lap joining. Compos Part B Eng 2015;73:82–8. doi:10.1016/j.compositesb.2014.12.029.

[18]   Santos TF de A, Torres EA, Ramirez AJ. Friction stir welding of duplex stainless steels. Weld Int 2017:1–9. doi:10.1080/09507116.2017.1347323.

[19]   Goushegir SM, dos Santos JF, Amancio-Filho ST. Influence of process parameters on mechanical performance and bonding area of AA2024/carbon-fiber-reinforced poly(phenylene sulfide) friction spot single lap joints. Mater Des 2015;83:431–42. doi:10.1016/j.matdes.2015.06.044. [20] Amancio-Filho ST. Friction Riveting: development and analysis of a new joining technique for polymer-metal multi-materials structures. Weld World 2011;55:13–24.

[21]   Amancio-Filho ST, Roeder J, Nunes SP, dos Santos JF, Beckmann F. Thermal degradation of polyetherimide joined by friction riveting (FricRiveting). Part I: Influence of rotation speed. Polym Degrad Stab 2008;93:1529–38. doi:10.1016/j.polymdegradstab.2008.05.019.

[22]   Borges MF, Amancio-Filho ST, dos Santos JF, Strohaecker TR, Mazzaferro JAE. Development of computational models to predict the mechanical behavior of Friction Riveting joints. Comput Mater Sci 2012;54:7–15. doi:10.1016/j.commatsci.2011.10.031.

[23]   Altmeyer J, dos Santos JF, Amancio-Filho ST. Effect of the friction riveting process parameters on the joint formation and performance of Ti alloy/short-fibre reinforced polyether ether ketone joints. Mater Des 2014;60:164–76. doi:10.1016/j.matdes.2014.03.042.

[24]   Blaga L, Bancilă R, dos Santos JF, Amancio-Filho ST. Friction Riveting of glass–fibrereinforced polyetherimide composite and titanium grade 2 hybrid joints. Mater Des 2013;50:825–9. doi:10.1016/j.matdes.2013.03.061.

[25]   Blaga L, dos Santos JF, Bancila R, Amancio-Filho ST. Friction Riveting (FricRiveting) as a new joining technique in GFRP lightweight bridge construction. Constr Build Mater 2015;80:167–79. doi:10.1016/j.conbuildmat.2015.01.001.

[26]   Rodrigues CF, Blaga LA, dos Santos JF, Canto LB, Hage E, Amancio-Filho ST. FricRiveting of aluminum 2024-T351 and polycarbonate: Temperature evolution, microstructure and mechanical performance. J Mater Process Technol 2014;214:2029–39. doi:10.1016/j.jmatprotec.2013.12.018.

[27]   Pagliarulo V, Palummo R, Rocco A, Ferraro P, Ricciardi MR, Antonucci V. Evaluation of delaminated area of polymer/Carbon Nanotubes fiber reinforced composites after flexural tests by ESPI. 2014 IEEE Metrol. Aerosp., IEEE; 2014, p. 211–5. doi:10.1109/MetroAeroSpace.2014.6865922.

[28]   Pagliarulo V, Rocco A, Langella A, Riccio A, Ferraro P, Antonucci V, et al. Impact damage investigation on composite laminates: comparison among different NDT methods and numerical simulation. Meas Sci Technol 2015;26:85603. doi:10.1088/0957-0233/26/8/085603.

[29]   Do V-T, Nguyen-Tran H-D, Chun D-M. Effect of polypropylene on the mechanical properties and water absorption of carbon-fiber-reinforced-polyamide-6/polypropylene composite. Compos Struct 2016;150:240–5. doi:10.1016/j.compstruct.2016.05.011.

[30]   Netz J, Hannemann B, Schmeer S. Micro-leveled modeling of structural stitched FRP joints as energy absorbing rupture points. Compos Struct 2016;157:131–40. doi:10.1016/j.compstruct.2016.08.026.

[31]   Njuguna, J, Mouti, Z, Westwood K. Influence of Temperature on Mechanical Properties of Short Glass Fibre-Reinforced Polyamide 6 and 66 Composites for Automotive Oil Pan Application. Light. Compos. Struct. Transp. Des. Manuf. Anal. Performance, 2016, p. 219.

[32]   http://www.matweb.com/ n.d. [33] Robnik-Šikonja   M,   Kononenko   I.   No Title.   Mach   Learn   2003;53:23–69. doi:10.1023/A:1025667309714.

[34]   Eriksson, L., Johansson, E., Kettaneh-Wold, N., Wikstrorn, C., Wold S. Design of Experiments Principles and Applications. 2000.

[35]   Zhang JZ, Chen JC, Kirby ED. Surface roughness optimization in an end-milling operation using the Taguchi design method. J Mater Process Technol 2007;184:233–9. doi:10.1016/j.jmatprotec.2006.11.029.